Geophysical Research Letters

Supporting Information for

Contributions of aerosol-cloud interactions to Mid-Piacenzian seasonally sea ice-free Arctic Ocean

Ran Feng[1,2*], Bette Otto-Bliesner[2], Yangyang Xu[3], Esther Brady[2], Tamara Fletcher[4,5], Ashley Ballantyne[4]

[1]Department of Geosciences, University of Connecticut, Storrs, CT 06269

[2]Paleo and Polar Climate Division, National Center for Atmospheric Research, 1850 Table Mesa Drive, Boulder, CO, 80305

[3]Department of Atmospheric Sciences, Texas A&M University, 400 Bizzell St, College Station, TX 77843

[4]W.A. Franke College of Forestry & Conservation, University of Montana, 32 Campus Dr, Missoula, MT 59812

[5]Institute of Applied Ecology, Chinese Academy of Sciences, Shenyang, China, 110016

Contents of this file

Introduction

The Supporting Information (SI) contains additional information on the model performance and experiments (text S1), adjusted effective radiative forcing of aerosols (text S2), figures that evaluate the performance of simulated clouds (Fig. S1), mean climate state of mid-Piacenzian (Fig. S2), and help explain the role of heat transport in simulated Arctic climate differences between Plio-Pristine and Plio-Polluted (Fig. S3 and S4).

Text S1. Model and Experiment Descriptions

The version of CESM1.2 used in this study is composed of Community Atmospheric Model version 5.3 (CAM5.3), Community Land Model version 4 (CLM4), Parallel Ocean

Program version 2 (POP2), and Community Ice CodE version 4 (CICE4). Different from previous versions of CAM, starting from CAM5.0, a two-moment (i.e., calculates both mixing ratio and number concentration) bulk microphysics scheme is linked to a 3-mode modular aerosol model (MAM3) to explicitly simulate ACI **[*Neale et al.*, 2010]**. This microphysics scheme solves for droplet activation and ice nucleation in clouds. MAM3 solves for sizes and number concentrations of internal mixtures of dust, sea-salt, sulfate, organics and black carbon using three categorical size bins of 0.02–0.08 μm (Aiken mode), 0.08–1 μm (Accumulation mode) and 1.0 – 10 μm (Coarse mode).

CAM5 simulates reasonable aerosol distributions **[*Liu et al.*, 2012]** and aerosol-cloud interactions **[*Gettelman*, 2015]** compared with observations and other models. But the model has a few known limitations and biases in representing ACI. First, the model does not explicitly simulate heterogeneous freezing on soot and on insoluble particles in mixed phase cloud, and cloud-borne aerosols in convective clouds **[*Neale et al.*, 2010]**. Second, the tropospheric concentration of black carbon and primary particulate organic matters are underestimated in the Arctic region **[*Liu et al.*, 2012]**. Finally, cloud radiative responses to aerosol changes are potentially too strong compared to observations **[*Malavelle et al.*, 2017]**. Nonetheless, as evaluated by previous studies **[*Kay et al.*, 2012]**, simulations of Arctic cloud cover by a slightly older version of CAM5 roughly agrees with Cloud-Aerosol Lidar and Infrared Pathfinder Satellite observations (CALIPSO). We repeated the same analysis using the embedded cloud simulator within CAM5.3 **[*Kay et al.*, 2012]** and forced with pre-industrial boundary conditions. Simulated total and low cloud fractions by CAM5.3 show reasonable agreement with CALIPSO especially in the North Atlantic and North Pacific (Fig. S1).

All simulations are run at 0.9×1.25° atmosphere and land resolution, and ~1° nominal ocean resolution. CCSM4-PlioMIP1**[*Rosenbloom et al.*, 2013]** is integrated for over 500 model years and has a top of the atmosphere (TOA) energy imbalance of <0.1 W/m^2. Both Plio-Pristine and Plio-Polluted are branched from CCSM4-PlioMIP1 at model year 500 from CCSM4-PlioMIP1, and are run for > 300 model years. At the end of the model runs, simulations reach a small TOA imbalance around 0.2 and 0.3 W/m^2 due to a small deep ocean (below 1 km) warming trend (Fig. S2a). For the final 100 model years of both runs, global mean surface temperature have negligible trends (< 0.1°C/century), both Arctic ice volumes and Atlantic Meridional Overturning Circulation are stable (<0.1% change per century) (Fig. S2b), suggesting quasi-equilibrium states in both simulations.

Finally, in order to quantify the Effective Radiative Forcing (ERF) from changes in aerosol emissions, we run two prescribed SST and sea ice experiments (pPlio-Pristine and pPlio-Polluted) using otherwise the same forcings and boundary conditions as Plio-Pristine and Plio-Polluted. Both experiments are run for 20 years and have reached small (<0.01°C/year) global surface temperature trends. The radiation diagnostics are calculated for the final 10 simulation years and averaged for both global and Arctic region (between 70° to 90°N).

Text S2. Adjusted Effective Radiative forcing (aERF)

According IPCC AR5 **[*Myhre et al.*, 2013]**, ERF is defined as the difference in the net TOA radiative fluxes (ΔTOA-R_{net}) between two prescribed SST and sea ice experiments. Based on definition, ERF should represent radiative changes induced by any forcing agents (tropospheric industrial pollutants in the current study) accounting for fast adjustments of clouds and water vapor but excluding responses from other components of climate system. However, we notice a strong surface albedo response in the Arctic region due to changes in land snow coverage despite the same prescribed SSTs and sea ice conditions in our experiments. Specifically, global and Arctic (70 – 90°N) surface albedo is lower in Plio-Pristine than Plio-Polluted with the same prescribed SST and sea ice from PlioMIP1-CCSM4 by 0.04% and 0.6% accounting for 0.1 W/m^2 and 0.9 W/m^2 increases in surface shortwave absorption (srf-ABS). We discount this effect by subtracting srf-ABS from the ΔTOA-R_{net} to attain an adjusted ERF (aERF), which only accounts for fast adjustments of clouds and water vapor.

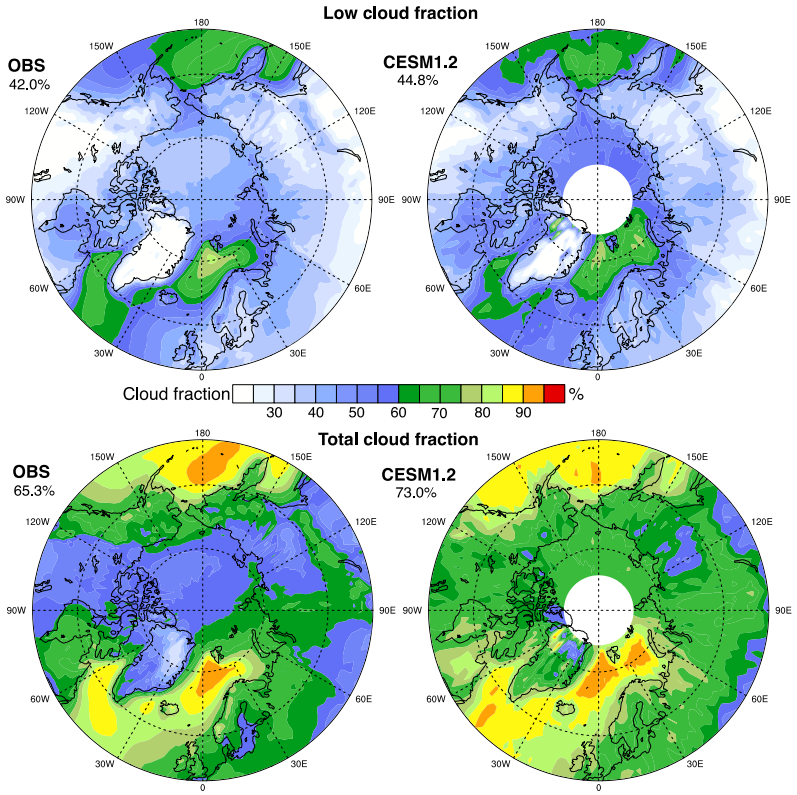

Figure S1. Observed (OBS) and simulated (CESM1.2) low and total cloud fraction of northern high latitudes. Observational data are from Cloud-Aerosol Lidar and Infrared Pathfinder Satellite observations (CALIPSO, Chepfer et al., 2008). CESM1.2 data are from a preindustrial simulation branched from a 1000-model year preindustrial simulation using a slightly older

model CESM1.1. The branched simulation uses preindustrial boundary conditions and is run for 300 model years, which allows the net top of the atmosphere radiation balance to drop below 0.1 W/m^2 for the final 100 model years. Numbers in the top left corners of each panel show the average cloud fraction between 50°N to 90°N.

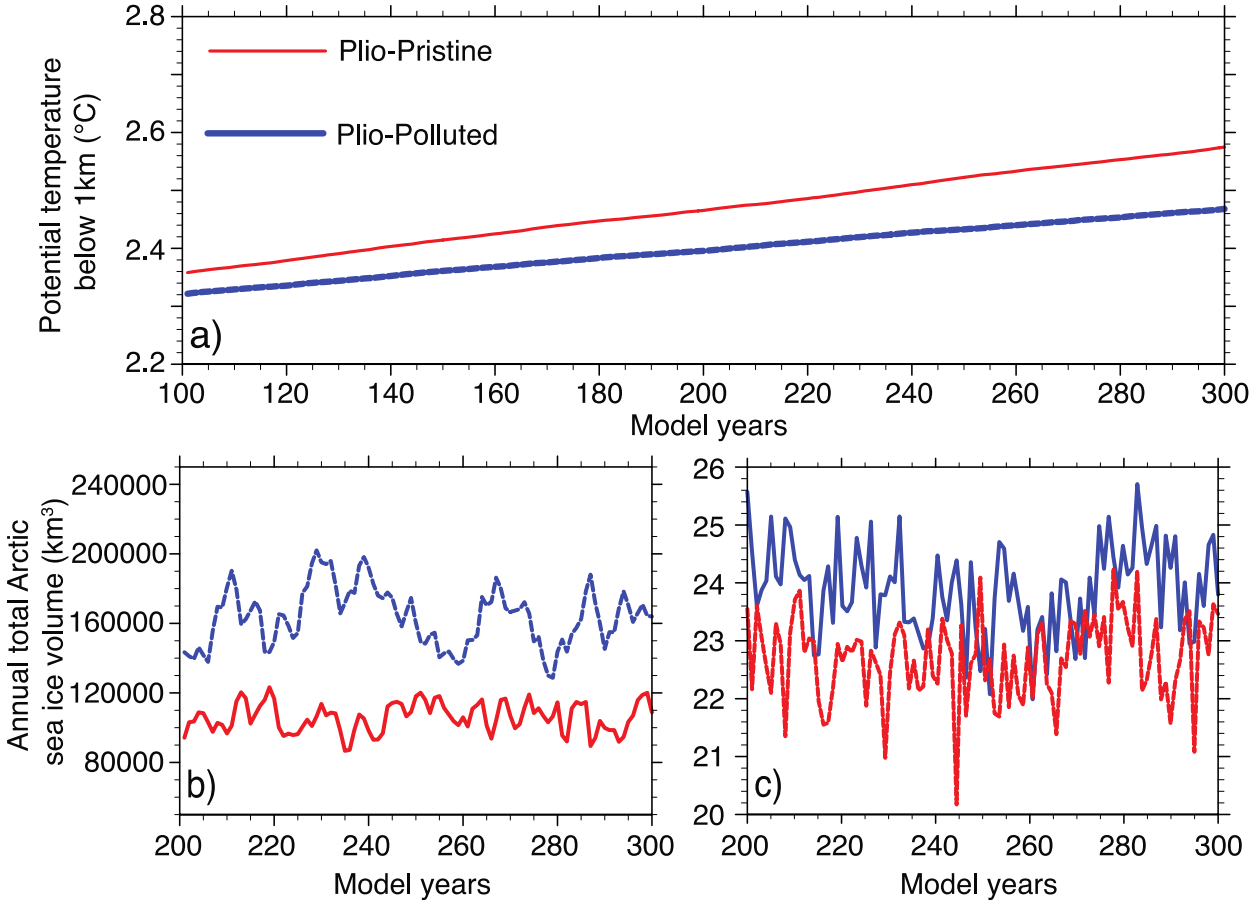

Figure S2. Time series of a) global mean deep ocean temperature of the last 200 model years, and b) annual total sea ice volumes of the northern hemisphere, and c) annual mean strength of Atlantic meridional overturning circulation (AMOC) during the last 100 model years in CESM1.2-Pristine and CESM1.2-Polluted. The AMOC strength is measured by the maximum of the meridional stream function north of 30°N and below 500 m within the Atlantic Ocean basin.

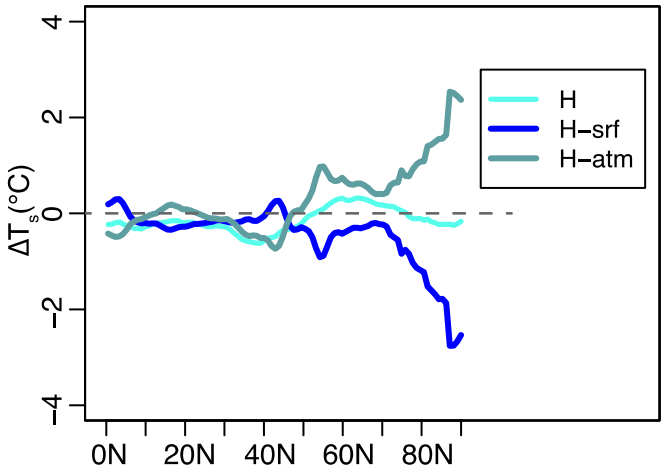

Figure S3. Surface temperature changes (ΔT_s) due to atmosphere (atm), surface (srf, including both ocean and ice), and total meridional heat convergence (H). Results are from the energy balance analysis.

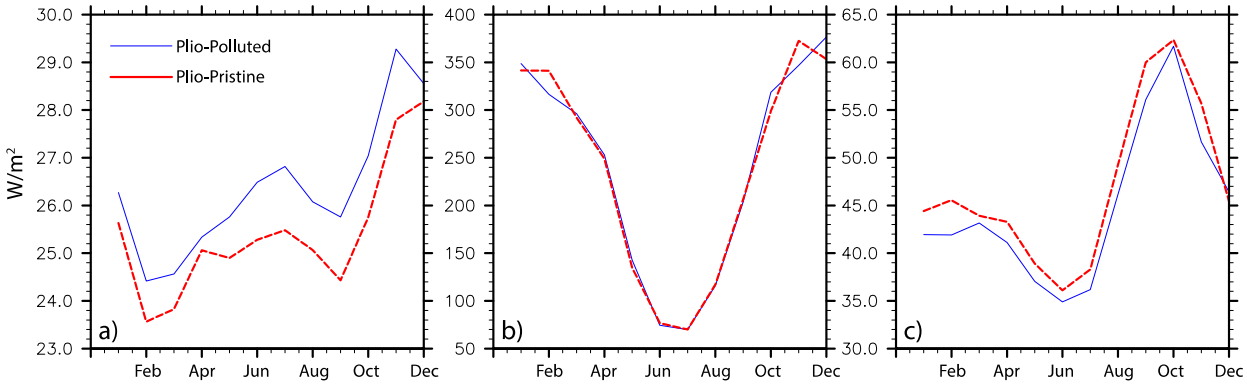

Figure S4. Contributions of monthly mean a) ocean, b) atmospheric specific and c) latent heat transport to northern high latitude radiation budget. The contributions are quantified by dividing northward heat transport at 60°N with the total surface area between 60°N and 90°N.

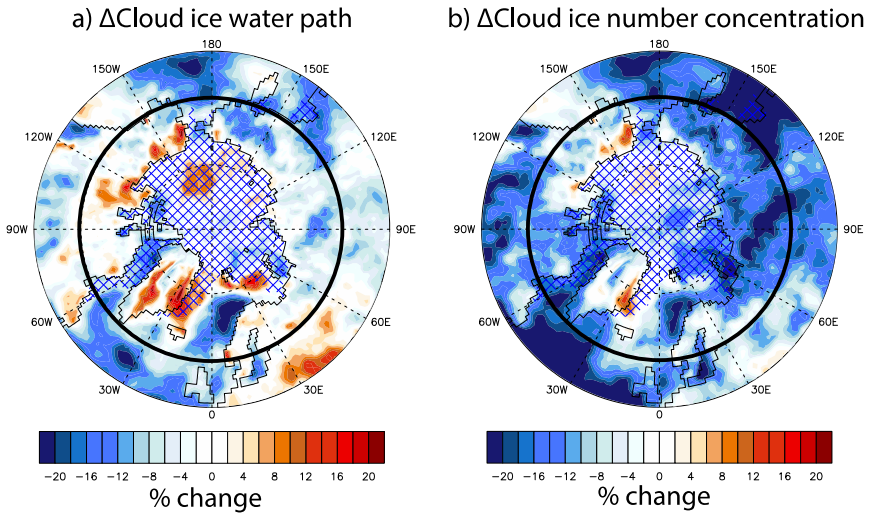

Figure S5. May to June average of % difference in a) cloud ice water path, and b) cloud ice number concentration integrated through the whole troposphere column between Plio-Pristine and Plio-Polluted. Bold solid line highlights the 60°N. Blue hatches show climatology of sea ice cover in Plio-Pristine.

References

Gettelman, A. (2015), Putting the clouds back in aerosol–cloud interactions, *Atmospheric Chemistry and Physics*, *15*(21), 12397–12411.

Kay, J. E., B. R. Hillman, S. A. Klein, Y. Zhang, B. Medeiros, R. Pincus, A. Gettelman, B. Eaton, J. Boyle, and R. Marchand (2012), Exposing global cloud biases in the Community Atmosphere Model (CAM) using satellite observations and their corresponding instrument simulators, *J. Climate*, *25*(15), 5190–5207.

Liu, X., R. C. Easter, S. J. Ghan, R. Zaveri, P. Rasch, X. Shi, J. F. Lamarque, A. Gettelman, H. Morrison, and F. Vitt (2012), Toward a minimal representation of aerosols in climate models: Description and evaluation in the Community Atmosphere Model CAM5, *Geosci. Model Dev.*, *5*(3), 709.

Malavelle, F. F., J. M. Haywood, A. Jones, A. Gettelman, L. Clarisse, S. Bauduin, R. P. Allan, I. H. H. Karset, J. E. Kristjánsson, and L. Oreopoulos (2017), Strong constraints on aerosol–cloud interactions from volcanic eruptions, *Nature*, *546*(7659), 485.

Myhre, G., D. Shindell, F.-M. Bréon, W. Collins, J. Fuglestvedt, J. Huang, D. Koch, J.-F. Lamarque, D. Lee, and B. Mendoza (2013), Anthropogenic and natural radiative forcing, *Climate change*, *423*, 658–740.

Neale, R. B., C.-C. Chen, A. Gettelman, P. H. Lauritzen, S. Park, D. L. Williamson, A. J. Conley, R. Garcia, D. Kinnison, and J.-F. Lamarque (2010), Description of the NCAR

community atmosphere model (CAM 5.0), *NCAR Tech. Note NCAR/TN-486+ STR*, *1*(1), 1–12.

Rosenbloom, N. A., B. L. Otto-Bliesner, E. C. Brady, and P. J. Lawrence (2013), Simulating the mid-Pliocene Warm Period with the CCSM4 model, *Geosci. Model Dev.*, *6*(2), 549–561, doi:10.5194/gmd-6-549-2013.